Anticancer Activity of BIM-46174, a New Inhibitor of the Heterotrimeric Gα/Gβγ Protein Complex

Grégoire P. Prévost,[1] Marie O. Lonchampt,[1] Susan Holbeck,[2] Samir Attoub,[3] Daniel Zaharevitz,[2] Mike Alley,[2] John Wright,[2] Marie C. Brezak,[1] Hélène Coulomb,[1] Ann Savola,[5] Marion Huchet,[1] Sophie Chaumeron,[1] Quang-Dé Nguyen,[3] Patricia Forgez,[3] Erik Bruyneel,[4] Mark Bracke,[4] Eric Ferrandis,[1] Pierre Roubert,[1] Danièle Demarquay,[1] Christian Gespach,[3] and Philip G. Kasprzyk[5]

[1]IPSEN-Institut Henri Beaufour, Les Ulis, France; [2]Developmental Therapeutics Program, Division of Cancer Treatment and Diagnosis, National Cancer Institute, Bethesda, Maryland; [3]Institut National de la Sante et de la Recherche Medicale U673, Université Pierre and Marie Curie, Paris-VI, Molecular and Clinical Oncology of Human Solid Tumors, Hôpital Saint-Antoine, Paris, France; [4]Laboratory of Experimental Cancerology, University Hospital, Gent, Belgium; and [5]IPSEN Albert Beaufour Research Institute, Milford, Massachusetts

Abstract

A large number of hormones and local agonists activating guanine-binding protein-coupled receptors (GPCR) play a major role in cancer progression. Here, we characterize the new imidazo-pyrazine derivative BIM-46174, which acts as a selective inhibitor of heterotrimeric G-protein complex. BIM-46174 prevents the heterotrimeric G-protein signaling linked to several GPCRs mediating (*a*) cyclic AMP generation (Gαs), (*b*) calcium release (Gαq), and (*c*) cancer cell invasion by Wnt-2 frizzled receptors and high-affinity neurotensin receptors (Gαo/i and Gαq). BIM-46174 inhibits the growth of a large panel of human cancer cell lines, including anticancer drug-resistant cells. Exposure of cancer cells to BIM-46174 leads to caspase-3-dependent apoptosis and poly(ADP-ribose) polymerase cleavage. National Cancer Institute COMPARE analysis for BIM-46174 supports its novel pharmacologic profile compared with 12,000 anticancer agents. The growth rate of human tumor xenografts in athymic mice is significantly reduced after administration of BIM-46174 combined with either cisplatin, farnesyltransferase inhibitor, or topoisomerase inhibitors. Our data validate the feasibility of targeting heterotrimeric G-protein functions downstream the GPCRs to improve anticancer chemotherapy. (Cancer Res 2006; 66(18): 9227-34)

Introduction

Emerging data show the involvement of guanine-binding protein-coupled receptors (GPCR) and their downstream signaling pathways in cancer progression (1–5). Growth of many cancers is stimulated by GPCR agonists, including vasoactive intestinal peptide (VIP), endothelin, neurotensin, thrombin, calcitonin gene-related peptide (CGRP), pituitary adenylyl cyclase–activating peptide, or growth hormone–releasing hormone (6–8). In addition to their effect on cancer cell proliferation, several GPCR agonists also activate the motility and invasive potential of transformed cells (CGRP, gastrin-releasing peptide, bombesin, neurotensin, and thrombin; refs. 9, 10). More recently, aberrant expression and activation of GPCRs and/or their associated G-proteins have been reported in human cancers (11). For example, constitutively active GPCR mutants harbor ligand-independent oncogenic properties as shown for the thyroid-stimulating hormone, luteinizing hormone (12), and cholecystokinin receptors (13). Moreover, activating mutations of the G-protein subunits αs, αi2, αi3, and β are reported as a putative cause of tumor formation (14, 15). Zeiger et al. (16) first showed *in vivo* that constitutive activation of Gα by a transgene expressing the cholera toxin A1 subunit in normal cells induced the mitotic activity, infiltration of skeletal muscle, and lung metastases. Recent research shows that Gβγ dimers are also involved in cancer transformation and invasive tumor growth because forced expression of Gβγ-sequestering agents, such as the COOH terminus of G-protein–coupled receptor kinase 2 (ct-βARK), obliterates multiple oncogenic pathways (17, 18). Conversely, overexpression of Gβγ subunits and constitutively active mutants of Gα subunits stimulates mitogen- and stress-activated protein kinase cascades p42/p44, p38, and c-Jun NH_2-terminal kinase, which regulate promoter activity of immediate response genes involved in cell proliferation, apoptosis, and transformation (19).

The biological effect of a given GPCR agonist is tentatively inhibited by a corresponding selective antagonist targeting the receptor (20–23). However, the therapeutic effect of this strategy should appear limited because tumor growth is simultaneously driven by several GPCR agonists. Following the binding of the GPCR agonist, the signal is transduced to the heterotrimeric G-protein complex, leading to its dissociation and liberation of activated GTP-bound Gα subunit and Gβγ dimers (4). Synthetic compounds and minigenes blocking heterotrimeric G-protein functions have been described previously (24–26). However, their potential therapeutic use is also limited due to their poor cell penetration and pharmacologic activity (26).

Here, we report the identification of BIM-46174, a novel synthetic small molecule inhibiting the heterotrimeric G-protein complex. Accordingly, BIM-46174 abrogates cancer cell invasion controlled by several GPCR agonists and inhibits cellular proliferation in a series of drug-resistant human cancer cell lines through caspase-3-dependent apoptosis. In addition, BIM-46174 exerts intrinsic antitumor activities and potentiates the activity of several classic anticancer agents in athymic mice bearing human lung and pancreatic cancer xenografts. Our data provide new insights into heterotrimeric G-proteins as targets for anticancer therapy using BIM-46174 alone or in combination with clinical anticancer drugs to limit the progression of advanced cancers.

Note: C. Gespach and P.G. Kasprzyk contributed equally to this work.

Requests for reprints: Grégoire P. Prévost, IPSEN-Institut Henri Beaufour, 5 Avenue du Canada, 91966 Les Ulis, France. Phone: 33-1-60-92-20-00; Fax: 33-1-69-07-38-02; E-mail: gregoire.prevost@ipsen.com.

doi:10.1158/0008-5472.CAN-05-4205

Materials and Methods

GPCR and signal transduction analysis. MCF-7 cancer cells were cultured at 37°C in 5% CO_2 humidified atmosphere using 96-well plates and DMEM containing 10% FCS, 1% glutamine, and antibiotics. After 4 days, cells were preincubated for 1 hour with BIM-46174. Then, cyclic AMP (cAMP)–inducing agents were added for a further 30-minute incubation period at 37°C. Intracellular cAMP levels were measured by RIA (kit SMP001A, NEN Life Science Products, Les Ulis, France). The EC_{50} and maximum effect (E_{MAX}) of activators were determined by computer-assisted nonlinear regression analysis (Data analysis toolbox, MDL Information Systems, Bourg La Reine, France). Intracellular calcium accumulation was measured by fluorescence assay according to the manufacturer (kit Calcium Plus, Molecular Devices, St. Gregoire, France). Data are expressed as relative fluorescence units.

Cell proliferation assay. Cell growth was determined by the WST1 colorimetric assay (Boehringer Mannheim, Meylan, Roche) as described previously (27). Briefly, cytotoxicity experiments were carried out at least thrice, each experiment representing eight determinations per concentration over the entire range. For each drug, the values included in the linear part of the sigmoid curve in each experiment were retained and a linear regression analysis was used to estimate IC_{50} values.

Cell cycle and apoptosis determination. FACStar+ flow cytometer (Becton Dickinson, Le Pont de Claix, France) was used to assess the change of cell cycle phase distribution and apoptosis induction as described previously (28). Briefly, cells were seeded at 0.5×10^6/5 mL culture medium in 25 cm^2 plastic flasks 24 hours before treatment. HL60 and NCI-H69 cells were then treated with drugs, and at selected time points, cells were harvested by centrifugation and washed twice in cold PBS. The cells were counted in a Beckman Z1 Coulter (Villepinte, France), fixed for 30 minutes at 4°C in 70% ethanol-PBS buffer, incubated with 50 μg/mL RNase A and 25 μg/mL propidium iodide or 5 μL Annexin V-FITC and 10 μL propidium iodide in binding buffer, and analyzed by two-color flow cytometry using a FACSCalibur cytometer.

Measure of cleaved caspase-3 and cleaved poly(ADP-ribose) polymerase. Meso Scale Discovery (MSD) biomarker detection assays were used to measure the amounts of cleaved caspase-3 and cleaved poly(ADP-ribose) polymerase (PARP) in cells following manufacturer's recommendations. Briefly, logarithmically growing HL60 (2.5×10^5 per well) and NCI-H69 (4×10^6 per well) cells were seeded in 12-well plate for 18 hours and then treated by BIM-46174 (30 μmol/L) for 6 and 24 hours, respectively. Whole-cell lysates (10 μg proteins) were added to MSD multiplex plate coated with an anticleaved PARP antibody and an anticleaved caspase-3 antibody. Both cleaved PARP and cleaved caspase-3 were revealed with one anti-PARP antibody and one anti-caspase-3 antibody labeled MSD Sulfo-TAG reagent. Inside the MSD instrument, a voltage applied to the plate electrode causes the labels bound to the electrode surface to emit light. The instrument measures intensity of the emitted light to afford a quantitative measure of the proteins of interest present in the samples issued of treated or untreated cells. All data are mean ± SE from at least two experiments.

Cellular invasion assay. Cancer cell invasion assays were done using collagen type I gels and parental or stably transfected colorectal, kidney, and lung cell lines as described previously (18, 29, 30). This assay is based on counting the percentage of invasive cells in collagen type I versus total number of viable cells in the same field. For each drug or agents at the concentrations used, it was systematically checked that none of them induced a loss of cell viability by trypan blue exclusion test during the 24-hour collagen invasion assay.

Growth of human cancer cell tumor xenografts. Human cancer cells (10^6) were s.c. injected into the flanks of female athymic NCr-*nu/nu* 4- to 6-week-old mice. Once the tumors (50-100 mm^3) were established, treatment was done by i.p. injections. Tumor volume measurements and animal weights were monitored two to three times weekly. Tumor volumes were calculated as described previously (31).

Results

Identification of BIM-46174 as an inhibitor of heterotrimeric G-protein complex. To identify selective inhibitors of heterotrimeric G-protein complex from our chemical library, we have developed a differential screening approach using human breast cancer MCF-7 cells as a model. In intact cells, the adenylyl cyclase effector generating cAMP from ATP can be stimulated indirectly by cholera toxin via ADP ribosylation and constitutive activation of the Gαs subunit, leading to activation of the plasma membrane–bound adenylyl cyclase. A second way to stimulate adenylyl cyclase is to use a direct adenylyl cyclase activator, the diterpene forskolin. Using this differential approach, pretreatment of cells with a potential heterotrimeric G-protein complex inhibitor should inhibit cholera toxin–induced cAMP generation but should be ineffective when adenylyl cyclase was directly activated by forskolin. We found that the imidazo-pyrazine derivative BIM-46174 (Fig. 1*A*) significantly decreased the potency EC_{50} of cholera toxin–induced cAMP generation without affecting the E_{MAX} = 78 ± 19 pmol/10^5 cells (Fig. 1*B*). Thus, BIM-46174 competitively inhibited cholera toxin–induced cAMP accumulation with a pA_2 value of 5.3 ± 0.05 (n = 5). In contrast, no effect on BIM-46174 was observed on cAMP generation promoted by the direct adenylyl cyclase activator forskolin even with high concentrations (100 μmol/L; Fig. 1*C*). To further assess the potential role of BIM-46174 as an inhibitor of heterotrimeric G-protein complex, its pharmacologic action has been challenged against adenylyl cyclase activation induced by one natural neuropeptide, VIP. The receptor of VIP is coupled to cAMP generation via the Gαs/Gβγ heterotrimeric complex in MCF-7 cells (32). As shown in Fig. 2*A*, preincubation of MCF-7 cells with BIM-46174 for 1 hour remarkably decreased the E_{MAX} of VIP (8 ± 1 pmol/10^5 cells) in a concentration-dependent manner (0-100 μmol/L BIM-46174) without affecting the VIP potency EC_{50} = 0.9 ± 0.1 nmol/L, showing that BIM-46174 is a noncompetitive inhibitor of VIP receptor with a pD'_2 value of 5.2 ± 0.04 (n = 4). In addition, the increase of preincubation time (0.5, 1, and 2.5 hours) with BIM-46174 (10 μmol/L) decreases the ratio of the E_{MAX} of VIP after preincubation over the E_{MAX} of VIP alone (63%, 45%, and 32%), respectively (data not shown). Inhibition of both cholera toxin– and VIP-induced cAMP generation by BIM-46174 was reversible on drug removal from the MCF-7 medium because cAMP levels could be recovered by 80% to 100% within 3 to 4 hours following a washout step (data not shown).

Because several GPCR agonists involved in cancer progression are linked to intracellular calcium translocation via the heterotrimeric protein complex Gαq/Gβγ, we next determined the effect of BIM-46174 on this cascade. As expected, BIM-46174 significantly reduced intracellular calcium translocation induced by the GPCR agonist endothelin-1 (ET-1) in human melanoma cells A2058 (Fig. 2*B*; ref. 33). Interestingly, when the intracellular calcium accumulation is induced by the G-protein–independent calcium ionophore A23187, the release was not affected by BIM-46174 (Fig. 2*B*).

Effect of BIM-46174 on cancer cell invasion induced by GPCR agonists and Gα/Gβγ subunits. Deregulated tumor cell growth, survival, and acquisition of the invasive phenotype are the hallmark of cancer progression. It was therefore of interest to determine whether BIM-46174 could inhibit cancer cell invasion induced by the Wnt oncogenic pathway that is directly connected with the heterotrimeric G-proteins Gαo/i and Gβγ (30). Treatment of HCT8/S11-Wnt-2 cells with either BIM-46174, the Gαo/i inhibitor pertussis toxin, the Gβγ-sequestering agent ct-βARK, or the phosphatidylinositol 3-kinase (PI3K) inhibitor wortmannin significantly abrogated the invasive potential of these

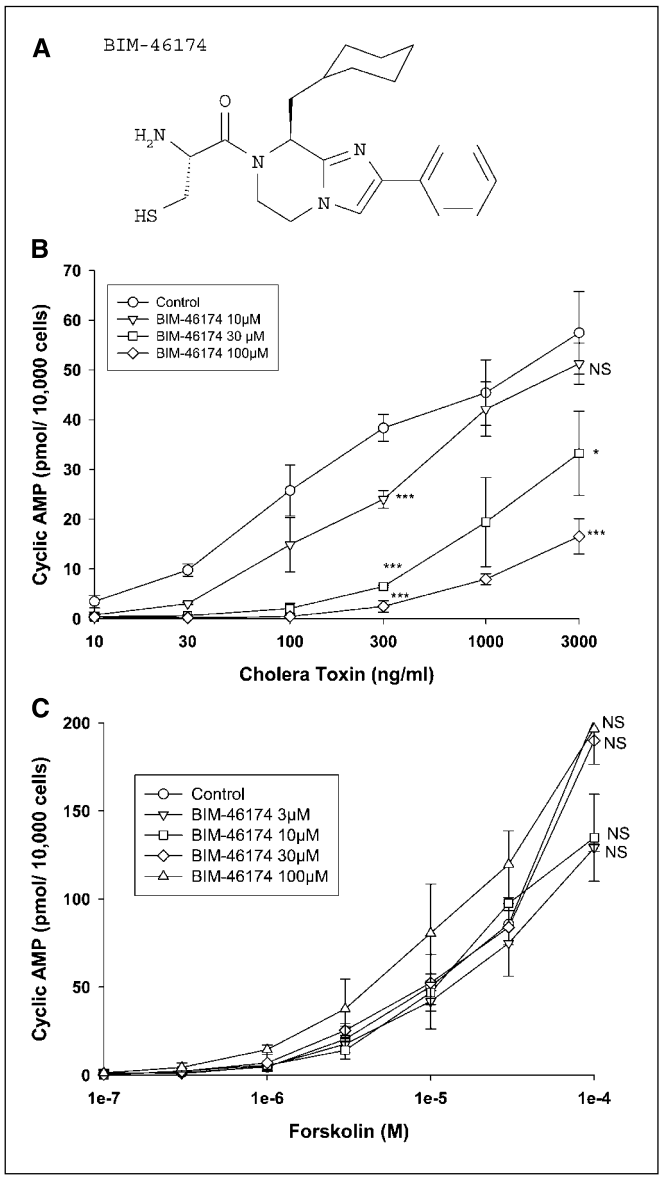

Figure 1. BIM-46174 only affects cAMP generation induced by cholera toxin via Gαs and not by forskolin directly acting on adenylyl cyclase. *A,* chemical structure of the new imidazo-pyrazine derivative BIM-46174. *B,* increasing concentrations of BIM-46174 inhibit cAMP generation induced by the direct activator of the Gαs subunit cholera toxin in the MCF-7 human breast cancer cell line. *C,* increasing concentrations of BIM-46174 do not inhibit cAMP generation induced by the direct adenylyl cyclase activator forskolin in the MCF-7 human breast cancer cell line. Statistical analyses have been done by comparison of groups in relation to the control group (*Control*) with a one-way ANOVA followed by Dunnett's tests. *NS,* not significant.

Wnt-2-transformed human colon cancer cells in collagen type I (Fig. 2*C*). We also activated HCT8/S11 invasiveness by external addition of the Wnt pathway agonist Wnt-3a and observed similar reversion by BIM-46174 and pertussis toxin (data not shown). In addition to these Wnt agonists (30), autocrine and paracrine mechanisms involving other GPCRs modulate the cell migration (34). To lend further support to our functional studies, we focused on the proinvasive loop determined by neurotensin in the metastatic human lung cancer cell line LNM35. Both neurotensin receptor antagonist SR48692 and BIM-46174 (IC_{50}, 0.7 μmol/L) completely reversed this constitutive invasive phenotype (Fig. 3*A*). A neurotensin neutralizing antibody produced the same inhibitory effect (data not shown). On the other hand, collagen invasion by human colon cancer cells HT29 can be induced by addition of exogenous neurotensin (EC_{50}, 8 nmol/L; Fig. 3*B*). As expected, such invasion is significantly blocked by BIM-46174. This pharmacologic response correlated with the ability of BIM-46174 and the nonhydrolysable GTP analogue GppNHp to displace the binding of labeled neurotensin to HT29 cell membranes, a property commonly described for GPCR coupled with Gα subunit (data not shown). In such 24-hour cell invasion assay, the concentrations of BIM-46174 used are not associated with alterations of cell viability by the trypan blue exclusion test. In agreement, the effective concentrations of BIM-46174 to reverse collagen invasion were much lower than the concentrations needed to induce significant apoptosis after 72-hour drug treatment (see below).

BIM-46174 has no effect on cancer cell invasion induced by individual subunits of heterotrimeric G-protein complex: Gα12, Gα13, or Gβ1γ2 dimer. BIM-46174 has no effect on the invasive potential of MDCKts.src cells (35) stably transfected by constitutively activated forms of either Gα12* or Gα13* subunits (GTPase-deficient mutants) or by forced expression of the Gβ1γ2 dimer (Fig. 3*C*; ref. 18). As well, BIM-46174 was ineffective against invasion induced by the G-protein–independent constitutively activated lipid protein kinase PI3K p110α (p110*). Next, we examined the effect of BIM-46174 on HCT8/S11 colon cancer cell invasion induced by aluminium fluoride ($AlF4^-$). $AlF4^-$ is an activator of the complex formed by the GDP-bound Gα subunit associated with G-protein βγ subunits. By mimicking the γ-phosphate of Gα-GTP, $AlF4^-$ initiates a cascade leading to Gα subunit activation and intracellular calcium elevation (36). $AlF4^-$ caused marked collagen invasion by HCT8/S11 cells (Fig. 3*D*), a cellular response that is completely reversed by BIM-46174.

Inhibitory effect of BIM-46174 on the *in vitro* proliferation of human cancer cells. The antiproliferative activity of BIM-46174 has been measured after a protracted exposure (96 hours) of human cancer cell lines established from nine tumor sites. The potency of BIM-46174 (IC_{50} values) ranged from 0.6 to 25 μmol/L (Table 1). The antiproliferative activities of BIM-46174 are depending on the time treatment of exposure. For example, on MIA PaCa-2 cells, the IC_{50} values, measured at 72 hours after the initiation of the treatment, are 34, 22, 14, and 10 μmol/L when BIM-46174 is applied for 3, 6, 9, or 72 hours. It is noteworthy that BIM-46174 was also active on several drug-resistant cell lines irrespective of the resistance mechanism involved, including drug extrusion (HL60DNR and HL60ADR) and alteration of the specific targets: topoisomerases (TOPO-II in HL60/MX2, TOPO-I in CCRF-CEM/C2) and glutathione *S*-transferase (NCI-H69/CPR). Most interesting, the resistance factors were much lower for BIM-46174 versus the reference drugs Adriamycin, daunorubicin, etoposide (VP-16), mitoxantrone (DHAD), and cisplatin (Table 1).

BIM-46174 classified as National Cancer Institute COMPARE-negative compound. To ensure the novelty of the proposed mechanism of action leading to cancer cell growth inhibition, BIM-46174 has been evaluated in the National Cancer Institute (NCI) COMPARE assay (37, 38). The NCI screens compounds for their ability to inhibit the growth of 60 human cancer cell lines in culture. Compounds with different mechanism of cell growth inhibition show different patterns of activity in the NCI screen. BIM-46174 (NSC727584) exhibited antiproliferative activities at the micromolar range on all 60 cell lines (data not shown). No

correlation was found in COMPARE analysis between BIM-46174 and 12,000 active compounds (Pearson correlation coefficient, >0.5). This database includes compounds acting through different mechanisms, such as DNA-damaging drugs, antimetabolites, tubulin- and cytoskeleton-interacting molecules, as well as signal transduction modulators. This lack of correlation suggests that BIM-46174 is acting through a novel inhibitory mechanism on the growth of several human cancer cell lines originating from nine different tumor sites.

Effect of BIM-46174 on the cell cycle and the apoptosis. No major change was observed in the percentage of HL60 and NCI-H69 cancer cells at the different phases of the cell cycle after 72 hours of treatment with 30 μmol/L BIM-46174 (Fig. 4*A*). In contrast, cisplatin treatment for 72 hours induced a clear increase of the percentage of lung NCI-H69 cells at the G_2 phase of the cell proliferation cycle. However, shorter exposure (24 and 48 hours) with BIM-46174 should lead to an increase of the G_2 phase (data not shown). Using Annexin V staining and flow cytometry, we assessed whether the antiproliferative activity of BIM-46174 is associated with alterations in HL60 and NCI-H69 cancer cell survival. Treatment with 30 μmol/L BIM-46174 for 72 hours resulted in a significant 5-fold increase in apoptosis in both cancer cell types (Fig. 4*B*). In contrast, cisplatin treatment for 72 hours did not induced significant apoptosis. Such cellular response to BIM-46174 is associated with a caspase-3 activation (Fig. 4*C*) and an appearance of cleaved PARP in both cell lines (Fig. 4*C*). Activation of caspase-8 and caspase-9 in HL60 cells is observed in cells treated with staurosporine but not by BIM-46174 (data not shown). To confirm the effect of such apoptosis induced by BIM-46174 after a short exposure, we have used the *in vitro* concentration × time assay, allowing the determination of BIM-46174 concentration and exposure time that produce growth inhibition and/or cell death (39). Initial experiments comparing several cancer cell lines issued from different tissues identified small cell lung cancer (SCLC) cells as BIM-46174 highly sensitive model system (data not shown). For more in-depth evaluation, five lung cancer cell lines and one human myeloma were selected, showing that growth inhibition (GI_{50}, total growth inhibition) and cell kill (LC_{50}) indices are achievable after 6 and 144 hours of exposure by low micromolar concentration. The protracted schedule gave slightly lower index values than short-term exposure (6 hours; data not shown).

BIM-46174 enhances the activity of anticancer drugs against human cancer cell xenografts. Figure 5 shows the activity of BIM-46174 alone or combined with standard anticancer drugs against the growth of tumor xenografts established from lung cancer cells NCI-H69 (SCLC), LNM35 [non-SCLC (NSCLC)], and pancreatic cancer cells MIA PaCa-2. The DNA-damaging agent cisplatin currently approved for clinical use against lung cancer has been evaluated *in vivo* in both lung xenograft models (Fig. 5*A* and *B*). Combined treatment of BIM-46174 with cisplatin induced a drastic reduction of the tumor growth rate in both SCLC (P = 0.018 at day 48) and NSCLC (P = 0.05) xenografts. The results of combinations of BIM-46174 with either the farnesyltransferase

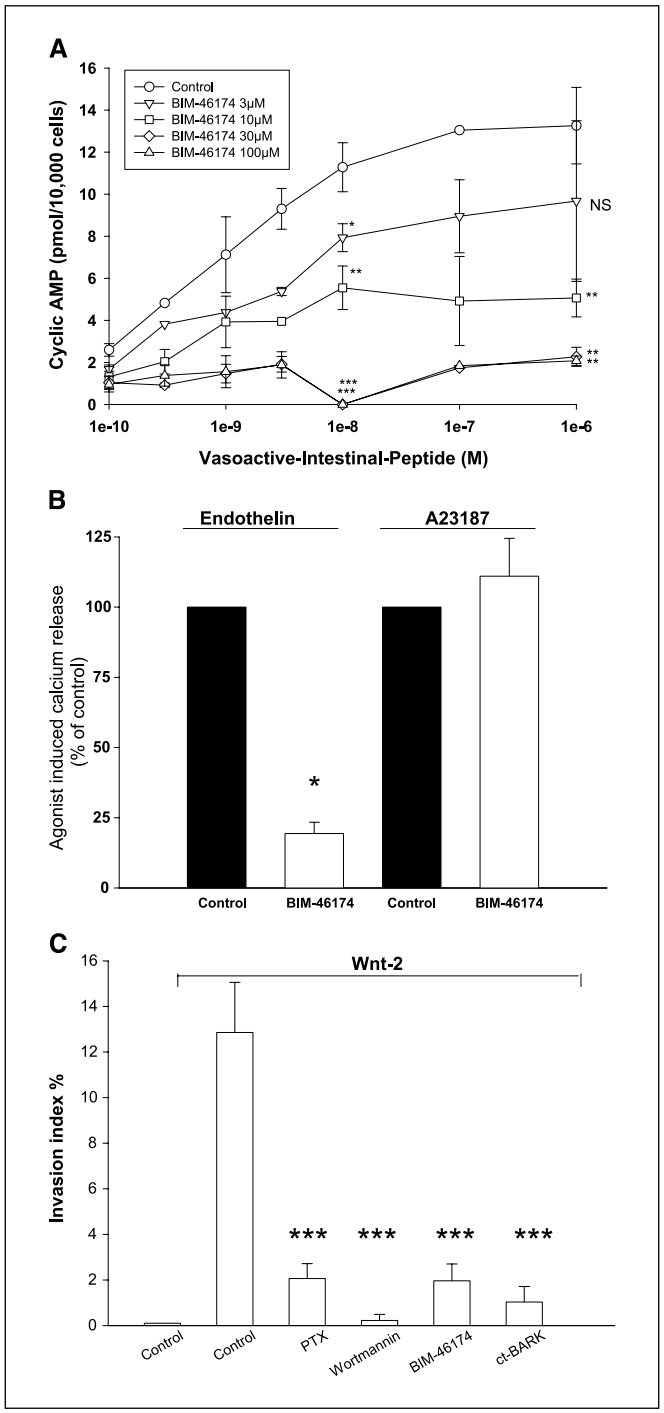

Figure 2. Effect of BIM-46174 on GPCR agonist-dependent signalization: cAMP synthesis, intracellular calcium release, and cell migration. *A,* increasing concentrations of BIM-46174 inhibit cAMP generation induced by increasing concentrations of VIP showing a noncompetitive inhibition. Statistical analyses have been done by comparison of groups in relation to the control group (*Control*) with a one-way ANOVA followed by Dunnett's tests. *B,* BIM-46174 (30 μmol/L) selectively inhibits Ca^{2+} release induced by the GPCR agonists: ET-1 (10 nmol/L) in melanoma cells A2058. In contrast, the same concentration of BIM-46174 was ineffective on Ca^{2+} release induced by the G-protein–independent Ca^{2+} ionophore A23187 (1 μmol/L) in the same cells A2058. Statistical analyses have been done by comparison of the mean in relation to the constant 100 with a Student's *t* test with a Benjamini-Hochberg adjustment for multiple comparisons. *C,* induction of collagen type I invasion by the forced expression of Wnt-2 in human colon cancer cells HCT8/S11-Wnt-2 (clones 3 and 8) and its reversion by the Gαo/i subunits inhibitor pertussis toxin (*PTX*; 200 ng/mL), the Gβγ scavenger, BIM-46174 (5 μmol/L), and the PI3K inhibitor wortmannin (10 nmol/L). The percentage of cells that invaded type I collagen gels is measured after a 24-hour period following the addition of the indicated effectors. Statistical analyses have been done by comparison of groups in relation to the control group (*Control*) with a one-way ANOVA followed by Dunnett's tests.

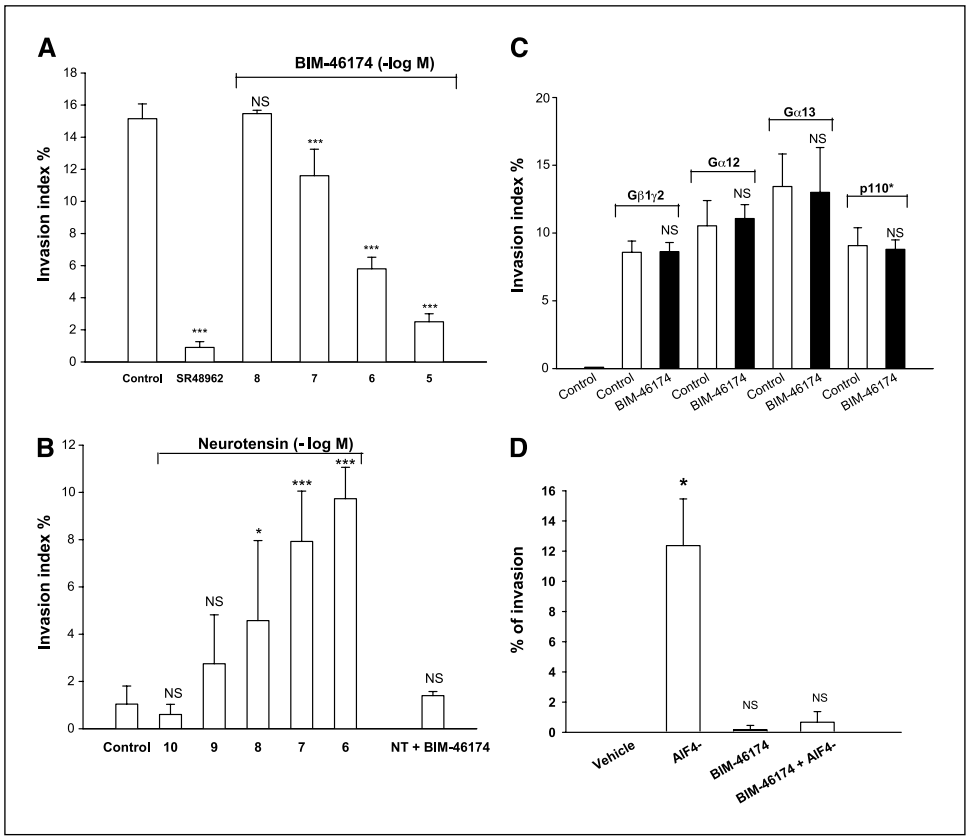

Figure 3. Effect of BIM-46174 on cancer cell invasion induced by GPCR agonists or by individual components of heterotrimeric G-proteins. *A,* disruption of the neurotensin autocrine proinvasive loop by increasing concentration of BIM-46174 or by the neurotensin receptor antagonist SR48692 (10 μmol/L) in human lung cancer cells LNM35. *B,* induction of the invasive phenotype of human HT29 colon cancer cells by external addition of neurotensin (*NT*) and its reversion (neurotensin, 1 μmol/L) by BIM-46174 (5 μmol/L). *C,* absence of BIM-46174 effect on the migration of MDCKts.src kidney cancer cells stably transfected by either constitutively activated Gα12* (clones 1 and 4) or Gα13* (clones 2 and 3) or p110α* (clone 2) or the Gβ1γ2 dimers (clones 4 and 11). Cells were incubated at the nonpermissive temperature 40°C for src activation in the presence or absence of BIM-46174 (5 μmol/L). *D,* for the 24-hour invasion assay, activation of the heterotrimeric complex was induced by $AlF4^-$ (5 mmol/L NaF and 100 μmol/L $AlCl_3$) in HCT8/S11 colon cancer cells preincubated for 1 hour in the presence or absence of BIM-46174 (5 μmol/L). Statistical analyses have been done by comparison in relation to the control group (*Vehicle*) with a paired Student's *t* test.

inhibitor BIM-46256 (40) against SCLC xenografts or the topoisomerase inhibitor BN80927 (28) against pancreatic MIA PaCa-2 xenografts are shown in Fig. 5*C* and *D*, respectively. In both cases, BIM-46174 in combination with farnesyltransferase inhibitor (P = 0.006 at day 21) or topoisomerase inhibitor (P < 0.001 at day 55) show significant antitumor activity. For all combinations, a limited body weight loss was observed in all groups. In terms of preliminary toxicity assessment, no significant changes of the blood markers, including urea, creatinine, glycemia, γ-glutamyl transpeptidase, aspartate aminotransferase, and alanine aminotransferase were observed in rats receiving a continuous infusion of BIM-46174 (2 mg/kg/h for 6 days) delivered by Alzet (L'Abresle, France) osmotic minipumps (data not shown). This regimen can be considered as the highest dose before observing a significant weight loss.

Discussion

We report the novel and atypical pharmacologic profile of BIM-46174, an imidazo-pyrazine derivative inhibiting heterotrimeric G-protein complex. Addition of BIM-46174 to tumor cells inhibits critical functions involved in cancer progression, including cell proliferation, survival, and invasion. Accordingly, in drug combination, BIM-46174 causes growth rate reduction of human lung and pancreatic cancer xenografts. Such atypical mechanism of action is well supported by the NCI COMPARE analysis showing a cancer cell sensitivity profile never observed before with 12,000 anticancer agents evaluated in the NCI chemical library. About the molecular site of action for BIM-46174, we present here convergent evidences that this new compound targets heterotrimeric G-protein signaling by inhibiting the formation and/or dissociation of the Gα/Gβγ heterotrimeric complex as shown by several assays and tools (i.e., intracellular cAMP production, calcium translocations, cholera toxin, and $AlF4^-$). In agreement with this interpretation, BIM-46174 was ineffective in controlling the invasive phenotype induced by individually activated GTPase-deficient Gα12 and Gα13 subunits and forced expression of Gβ1γ2 dimers. To substantiate further the selective activity of BIM-46174 on large G-proteins, its activity was tested on non-GPCR signaling pathways, including Rho-like small GTPases, angiogenic tyrosine kinases, and other molecular intermediates acting downstream of GPCR-Gα/βγ complexes. In that respect, BIM-46174 was ineffective on (*a*) molecular interventions directly activating adenylate cyclase (forskolin; Fig. 1), (*b*) intracellular calcium levels induced by calcium ionophore A23187 (Fig. 2), (*c*) the constitutively active PI3K protein lipid kinase (p110α*; Fig. 3), (*d*) the GTP-bound status of the active forms of the Rac1 and RhoA small GTPases (data not shown), and (*e*) the vascular endothelial growth factor (VEGF) and fibroblast growth factor (FGF) tyrosine kinase receptors driven angiogenesis in human umbilical vascular endothelial cell (HUVEC; data not shown).

Deregulation of cell proliferation and survival is commonly accepted as an initial transforming mechanism leading to the neoplastic progression at the proliferation/differentiation interface. Here, the antiproliferative activities of BIM-46174 are observed in several cancer types *in vitro*, including five drug-resistant models. This activity against drug-resistant cancer cell lines is an important property because drug resistance clearly remains one of the primary causes of suboptimal outcomes in cancer therapy. As BIM-46174 is characterized in the NCI COMPARE assay with an original antiproliferative profile, this supports the thought that BIM-46174 is acting on proliferative/survival signaling pathways through a

Table 1. Antiproliferative activity of BIM-46174 on a series of human cancer cells in culture, including drug-resistant tumor cell lines

Cell lines	Cell types	IC_{50} of BIM-46174 (μmol/L)
A-427	Lung	0.6
LNCaP	Prostate	1.3
HL60	Leukemia	2.3
HEK-293	Embryo kidney	7.8
CCRF-CEM	Leukemia	9
Mia PaCa-2	Pancreas	9.6
NCI-H69	SCLC	11.4
U-87MG	Glioma	12.7
A2058	Melanoma	14
HT29	Colon	17.7
DU145	Prostate	25
SKOV-3	Ovary	>25

Drug-resistant cells	Drugs	Resistance factor
HL60/HL60DNR	Daunorubicin	106
	BIM-46174	4.3
HL60/HL60ADR	Adriamycin	90
	BIM-46174	0.8
HL60/HL60/MX2	DHAD	6
	BIM-46174	0.8
NCI-H69/NCI-H69/CPR	Cisplatin	3.8
	BIM-46174	0.8
CCRF-CEM/C2	VP-16	11.3
	BIM-46174	1.4

NOTE: The inhibitory potency IC_{50} of BIM-46174 on cell proliferation was determined after a 96-hour protracted infusion of BIM-46174 during the exponential phase of growth. For drug-resistant cancer cells, the resistance factor is calculated by dividing the IC_{50} of BIM-46174 on the drug-resistant variant by the IC_{50} of BIM-46174 on parental cells. This ratio is compared with the resistance factors observed for reference anticancer drugs.

selective and original mechanism not targeted by 12,000 reference drugs (41). Interestingly, we found that the IC_{50} values of this compound on cell growth and invasion (0.6-25 μmol/L) are lower than the concentrations needed to block G-protein–activated cAMP accumulation and calcium release (30-100 μmol/L). Consistent with this observation, we clearly showed that BIM-46174 is acting on GPCR signaling controlled by several GPCR agonists mediating cell proliferation, survival, and invasion signals. In support with this mechanism, it is not surprising that this multitargeted GPCR drug exerts cumulative and potent actions on integrated cellular functions regulated by several heterotrimeric G-protein complex and transduction systems (cAMP, cyclic guanosine 3′,5′-monophosphate, calcium translocations, etc.). The difference between IC_{50}s observed in G-protein signaling assays and cell proliferation is explained by the fact that the G-protein signaling assays are done on cells exposed to BIM-46174 for only a short period (0.5-1 hour), whereas the antiproliferation assays are done after a longer 96-hour exposure. Our findings on the cell cycle suggest that the anticancer efficacy of BIM-46174 is not only mediated via a G_2 arrest because this blockade is no longer observed with protracted treatment. Biochemical analyses revealed that BIM-46174 induced cancer cell death through caspase-3-dependent apoptotic pathway leading to a PARP cleavage with an absence of caspase-8 and caspase-9 activation. Further in-depth characterization of the apoptotic pathways targeted by BIM-46174 should be pursued to complete this first approach because GPCRs are involved in cell survival and cytoprotection either directly or indirectly through transactivation or reciprocal cross talk with receptor and nonreceptor kinases (42). However, it is noteworthy that the experimental variables (time and concentration) to observe apoptosis

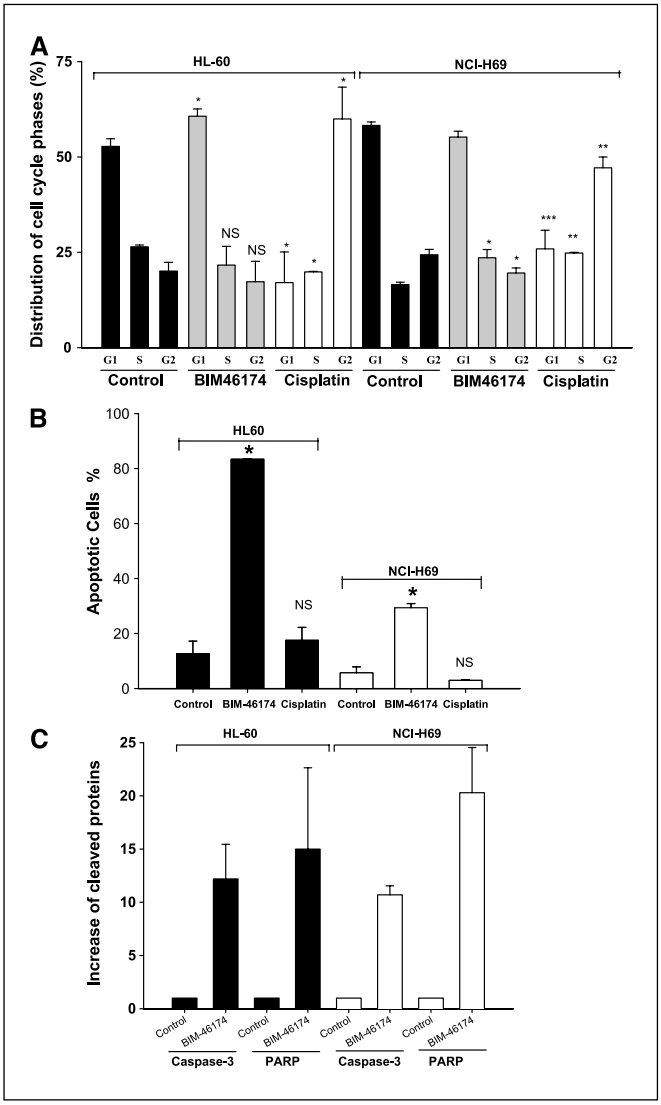

Figure 4. Effect of BIM-46174 on the cell proliferation cycle, cell survival, caspase-3 activity, and PARP cleavage in HL60 and NCI-H69 cancer cells. *A,* assessed by fluorescence-activated cell sorting (FACS) analysis, BIM-46174 (30 μmol/L, 72 hours of exposure) had no major effect on cancer cell distribution in the different phases of the cell cycle. Statistical analyses have been done by comparison of groups in relation to the control group (*Control*) with a one-way ANOVA followed by Dunnett's tests. *B,* apoptosis is induced in both cancer cell lines by BIM-46174 assessed by FACS analysis and Annexin V labeling. In contrast, cisplatin increased the percentage of cancer cells in G_2 phase without effect on apoptosis. Statistical analyses have been done by comparison in relation to the control group (*Vehicle*) with a paired Student's *t* test. *C,* BIM-46174 (30 μmol/L) increases cleaved caspase-3 and cleaved PARP in both cell lines. *Columns,* mean of three experiments for 6-hour exposure of BIM-46174; *bars,* SE.

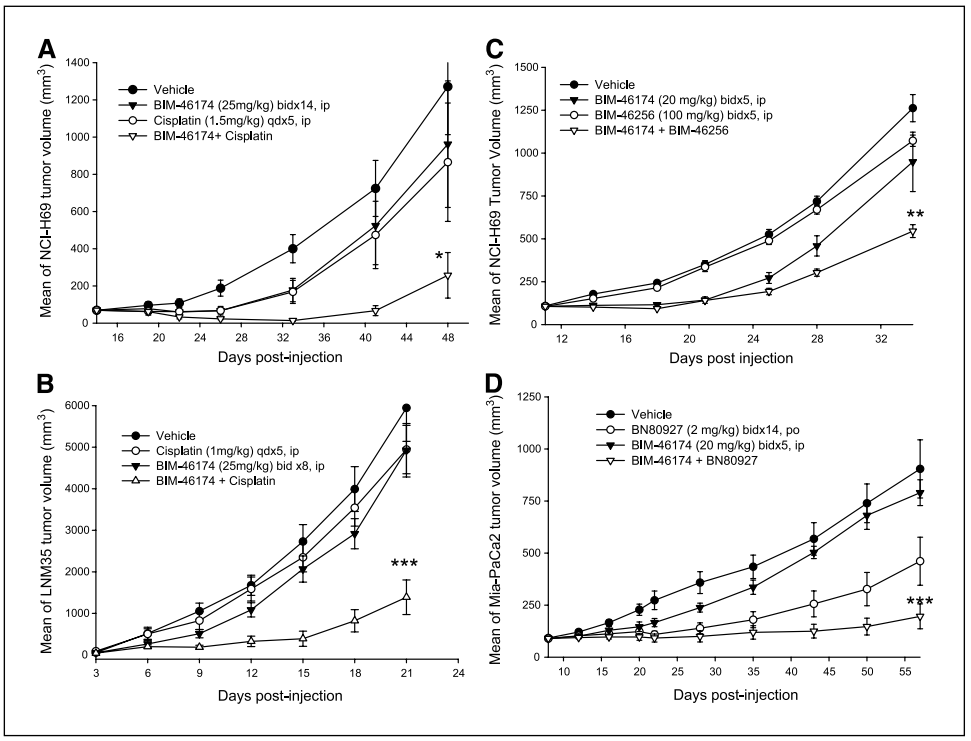

Figure 5. Antitumor activity of BIM-46174 alone or in combination with anticancer drugs against human lung and pancreatic tumor xenografts in athymic nude mice. *A* and *B*, BIM-46174 enhances cisplatin efficacy against SCLC NCI-H69 and NSCLC LNM35 cells growing as xenografts. *C*, BIM-46174 enhances the efficacy of the farnesyltransferase inhibitor BIM-46256 against SCLC NCI-H69 tumor xenografts. *D*, BIM-46174 enhances the efficacy of the topoisomerase inhibitor BN80927 against pancreatic cancer MIA PaCa-2 xenografts. For all combinations, a minimal toxicity with a limited body weight loss was observed in all groups. Statistical analyses have been done by comparison of groups in relation to the control group (*Control*) with a one-way ANOVA followed by Dunnett's tests.

are in line with the time required to observe cell killing in the time × concentration assay. This pharmacologic signature is compatible with our data, showing that BIM-46174 may improve the therapeutic effect of anticancer agents against human lung and pancreatic cancer cells characterized by various forms of drug resistance.

More advanced cancers are characterized by local malignant recurrences after surgery and adjuvant therapy and synchronous and metachronous metastases in different organs. A myriad of GPCR agonists, such as cyclooxygenase-2-derived eicosanoids, CXC chemokines, hormones, and neuropeptides, play a key role in cancer cell motility and invasive behavior, tumor angiogenesis, and homing survival of metastatic cancer cells in distant organs. In addition to their direct mitogenic and invasion-promoting effects, GPCR agonists, including bombesin, endothelin, and thrombin protease-activated receptor-1 receptors, also indirectly promote metalloproteinase-mediated cleavage of epidermal growth factor receptor (EGFR) ligand precursors and EGFR transactivation (43, 44). Although BIM-46174 has no effect on the angiogenic responses induced by the VEGF and FGF tyrosine kinase receptors in normal primary endothelial cells HUVEC (data not shown), its potential effect on tumor angiogenesis promoted by GPCR agonists should be still considered *in vivo*. Our data show that BIM-46174 inhibits G-protein signaling and the invasive phenotype determined in cancer cells by several GPCRs.

Combination therapy using anticancer agents acting through different mechanisms is a current strategy in clinical chemotherapy to identify optimal regimens in terms of patient survival and relapse-free disease. Both pancreatic and lung cancers (SCLC and NSCLC), leading causes of mortality worldwide, are considered as particularly aggressive and respond poorly to standard treatments. The survival rate for these malignancies is very low because less than 4% to 10% survival benefit occurred at 5 years after adjuvant therapy. Our data show that BIM-46174 collaborates with cisplatin, farnesyltransferase, or topoisomerase inhibitors in delaying the growth of human lung and pancreatic tumor xenografts in athymic mice. Although the molecular mechanisms involved in such interactions have not been completely identified, a clear benefit has been observed in these preclinical models. Additional types of tumor sites have to be evaluated with BIM-46174, especially hormonotherapy refractory prostate cancers (45) and neuroendocrine tumors characterized by the production of peptide hormones, bioamines, and neurotransmitters acting through GPCR agonist-mediated autocrine loops.

Taken together, our data bring robust evidence that targeting heterotrimeric G-protein signaling represents a promising new strategy for anticancer therapy. The design and characterization of BIM-46174 as a first generation of heterotrimeric signaling G-protein inhibitors validate such an approach.

Acknowledgments

Received 12/13/2005; revised 6/22/2006; accepted 7/11/2006.

The costs of publication of this article were defrayed in part by the payment of page charges. This article must therefore be hereby marked *advertisement* in accordance with 18 U.S.C. Section 1734 solely to indicate this fact.

References

1. Gutkind JS. Cell growth control by G protein-coupled receptors: from signal transduction to signal integration. Oncogene 1998;17:1331–42.
2. Yowell CW, Daaka Y. G protein-coupled receptors provide survival signals in prostate cancer. Clin Prostate Cancer 2002;21:177–81.
3. Regnauld K, Nguyen QD, Vakaet L, et al. G-protein αolf subunit promotes cellular invasion, survival, and neuroendocrine differentiation in digestive and urogenital epithelial cells. Oncogene 2002;21:4020–31.
4. Cabrera-Vera TM, Vanhauwe J, Thomas TO, et al. Insights into G protein structure, function, and regulation. Endocr Rev 2003;24:765–81.

5. Nguyen QD, Faivre S, Bruyneel E, et al. RhoA- and RhoD-dependent regulatory switch of Gα subunit signaling by PAR-1 receptors in cellular invasion. FASEB J 2002;16:565–76.
6. Kiaris H, Schally AV, Varga JL, Groot K, Armatis P. Growth hormone-releasing hormone: an autocrine growth factor for small cell lung carcinoma. Proc Natl Acad Sci U S A 1999;96:14894–8.
7. Bepler G, Zeymer U, Mahmoud S, et al. Substance P analogues function as bombesin receptor antagonists and inhibit small cell lung cancer clonal growth. Peptides 1988;9:1367–72.
8. Moody TW, Chan D, Fahrenkrug J, Jensen RT. Neuropeptides as autocrine growth factors in cancer cells. Curr Pharm Des 2003;9:495–509.
9. Rozengurt E. Neuropeptides as growth factors for normal and cancerous cells. Trends Endocrinol Metab 2002;13:128–34.
10. Rozengurt E. Autocrine loops, signal transduction, and cell cycle abnormalities in the molecular biology of lung cancer. Curr Opin Oncol 1999;11:116–22.
11. Sin WC, Zhang Y, Zhong W, et al. G protein-coupled receptors GPR4 and TDAG8 are oncogenic and overexpressed in human cancers. Oncogene 2004;23:6299–303.
12. Cotecchia S, Fanelli F, Costa T. Constitutively active G protein-coupled receptor mutants: implications on receptor function and drug action. Assay Drug Dev Technol 2003;1:311–6.
13. Gales C, Sanchez D, Poirot M, et al. High tumorigenic potential of a constitutively active mutant of the cholecystokinin 2 receptor. Oncogene 2003;22:6081–9.
14. Fragoso MC, Latronico AC, Carvalho FM, et al. Activating mutation of the stimulatory G protein (gsp) as a putative cause of ovarian and testicular human stromal Leydig cell tumors. J Clin Endocrinol Metab 1998;83:2074–8.
15. Radhika V, Dhanasekaran N. Transforming G proteins. Oncogene 2001;20:1607–14.
16. Zeiger MA, Saji M, Caturegli P, Westra WH, Kohn LD, Levine MA. Transformation of rat thyroid follicular cells stably transfected with cholera toxin A1 fragment. Endocrinology 1996;137:5392–9.
17. Bookout AL, Finney AE, Guo R, Peppel K, Koch WJ, Daaka Y. Targeting Gβγ signaling to inhibit prostate tumor formation and growth. J Biol Chem 2003;278:37569–73.
18. Faivre S, Regnauld K, Bruyneel E, et al. Suppression of cellular invasion by activated G-protein subunits Gαo, Gαi1, Gαi2, and Gαi3 and sequestration of Gβγ. Mol Pharmacol 2001;60:363–72.
19. Crespo P, Xu N, Simonds WF, Gutkind JS. Ras-dependent activation of MAP kinase pathway mediated by G-protein βγ subunits. Nature 1994;369:418–20.
20. Prevost G, Foehrle E, Thomas F, et al. Growth of human breast cancer cell lines is inhibited by the somatostatin analog BIM23014. Endocrinology 1991;129:323–9.
21. Prevost G, Mormont C, Gunning M, Thomas F. Therapeutic use and perspectives of synthetic peptides in oncology. Acta Oncol 1993;32:209–15.
22. Jungwirth A, Galvan G, Pinski J, et al. Luteinizing hormone-releasing hormone antagonist Cetrorelix (SB-75) and bombesin antagonist RC-3940-II inhibit the growth of androgen-independent PC-3 prostate cancer in nude mice. Prostate 1997;32:164–72.
23. Jungwirth A, Schally AV, Pinski J, et al. Inhibition of *in vivo* proliferation of androgen-independent prostate cancers by an antagonist of growth hormone-releasing hormone. Br J Cancer 1997;75:1585–92.
24. Breitweg-Lehmann E, Czupalla C, Storm R, et al. Activation and inhibition of G proteins by lipoamines. Mol Pharmacol 2002;61:628–36.
25. Beindl W, Mitterauer T, Hohenegger M, Ijzerman AP, Nanoff C, Freissmuth M. Inhibition of receptor/G protein coupling by suramin analogues. Mol Pharmacol 1996;50:415–23.
26. Freissmuth M, Waldhoer M, Bofill-Cardona E, Nanoff C. G protein antagonists. Trends Pharmacol Sci 1999;20:237–45.
27. Brezak MC, Quaranta M, Mondesert O, et al. A novel synthetic inhibitor of CDC25 phosphatases: BN82002. Cancer Res 2004;64:3320–5.
28. Demarquay D, Huchet M, Coulomb H, et al. BN80927: a novel homocamptothecin that inhibits proliferation of human tumor cells *in vitro* and *in vivo*. Cancer Res 2004;64:4942–9.
29. Rodrigues S, Nguyen QD, Faivre S, et al. Activation of cellular invasion by trefoil peptides and src is mediated by cyclooxygenase- and thromboxane A2 receptor-dependent signaling pathways. FASEB J 2001;15:1517–28.
30. Le Floch N, Rivat C, De Wever O, et al. The proinvasive activity of Wnt-2 is mediated through a noncanonical Wnt pathway coupled to GSK-3β and c-Jun/AP-1 signaling. FASEB J 2005;19:144–6.
31. Prevost G, Lanson M, Thomas F, et al. Molecular heterogeneity of somatostatin analogue BIM-23014C receptors in human breast carcinoma cells using the chemical cross-linking assay. Cancer Res 1992;52:843–50.
32. Gespach C, Bawab W, de Cremoux P, Calvo F. Pharmacology, molecular identification, and functional characteristics of vasoactive intestinal peptide receptors in human breast cancer cells. Cancer Res 1988;48:5079–83.
33. Graham FL, Smiley J, Russell WC, Nairn R. Characteristics of a human cell line transformed by DNA from human adenovirus type 5. J Gen Virol 1977;36:59–74.
34. Souaze F, Viardot-Foucault V, Roullet N, et al. Neurotensin receptor 1 gene activation by the Tcf/β-catenin pathway is an early event in human colonic adenomas. Carcinogenesis 2006;27:708–16.
35. Gaush CR, Hard WL, Smith TF. Characterization of an established line of canine kidney cells (MDCK). Proc Soc Exp Biol Med 1966;122:931–5.
36. Satoh Y, Williams MR, Habara Y. Effects of $AlF4^-$ and ATP on intracellular calcium dynamics of crypt epithelial cells in mouse small intestine. Cell Tissue Res 1999;298:295–305.
37. Zaharevitz DW, Holbeck SL, Bowerman C, Svetlik PA. COMPARE: a web accessible tool for investigating mechanisms of cell growth inhibition. J Mol Graph Model 2002;20:297–303.
38. Paull KD, Shoemaker RH, Hodes L, et al. Display and analysis of patterns of differential activity of drugs against human tumor cell lines: development of mean graph and COMPARE algorithm. J Natl Cancer Inst 1989;81:1088–92.
39. Alley MC, Hollingshead MG, Pacula-Cox CM, et al. SJG-136 (NSC 694501), a novel rationally designed DNA minor groove interstrand cross-linking agent with potent and broad spectrum antitumor activity. Part 2: efficacy evaluations. Cancer Res 2004;64:6700–6.
40. Vicat JM, Ardila-Osorio H, Khabir A, et al. Apoptosis and TRAF-1 cleavage in Epstein-Barr virus-positive nasopharyngeal carcinoma cells treated with doxorubicin combined with a farnesyl-transferase inhibitor. Biochem Pharmacol 2003;65:423–33.
41. Coso OA, Montaner S, Fromm C, et al. Signaling from G protein-coupled receptors to the c-jun promoter involves the MEF2 transcription factor. Evidence for a novel c-jun amino-terminal kinase-independent pathway. J Biol Chem 1997;272:20691–7.
42. Li YM, Pan Y, Wei Y, et al. Upregulation of CXCR4 is essential for HER2-mediated tumor metastasis. Cancer Cell 2004;6:459–69.
43. Schafer B, Gschwind A, Ullrich A. Multiple G-protein-coupled receptor signals converge on the epidermal growth factor receptor to promote migration and invasion. Oncogene 2004;23:991–9.
44. Zhao D, Zhan Y, Koon HW, et al. Metalloproteinase-dependent transforming growth factor-α release mediates neurotensin-stimulated MAP kinase activation in human colonic epithelial cells. J Biol Chem 2004;279:43547–54.
45. Dai J, Shen R, Sumitomo M, Stahl R, et al. Synergistic activation of the androgen receptor by bombesin and low-dose androgen. Clin Cancer Res 2002;8:2399–405.

Anticancer Activity of BIM-46174, a New Inhibitor of the Heterotrimeric G α/G$\beta\gamma$ Protein Complex

Grégoire P. Prévost, Marie O. Lonchampt, Susan Holbeck, et al.

Cancer Res 2006;66:9227-9234.